

Short Note

# Bis(*N*-*tert*-butylacetamido)(dimethylamido)(chloro)titanium

 Dennis M. Seth, Jr. and Rory Waterman \* 

Department of Chemistry, University of Vermont, Burlington, VT 05405, USA

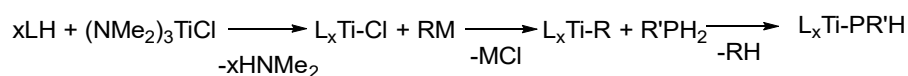
\* Correspondence: rory.waterman@uvm.edu; Tel.: +1-802-656-0278

**Abstract:** The titanium amidate compound bis(*N*-*tert*-butylacetamido)(dimethylamido)(chloro)titanium was synthesized by the protonolysis of tris(dimethylamido)(chloro)titanium and structurally characterized by  $^1\text{H}$  and  $^{13}\text{C}$  NMR spectroscopy as well as X-ray diffraction. The compound does not appear to react cleanly nor readily with routine alkylating agents such as *sec*-butyllithium, benzyl potassium, or trimethylsilyl methylolithium.

**Keywords:** titanium; amidate; crystal

## 1. Introduction

Hydrophosphination remains one of the most atom-economical and efficient ways of forming P–C bonds, though challenges still exist [1,2]. Catalytic hydrophosphination has been observed with many metals [3], though examples involving titanium are limited in both scope and conversion [4–6]. Previous work with triamidoamine-supported titanium compounds showed that while the alkyl derivative was active for catalytic hydrophosphination, the titanium phosphido derivative was inactive [7]. However, this compound was capable of undergoing insertion at the Ti–P bond with a variety of polar, unsaturated substrates. A developing hypothesis in this area is that a metal–phosphido compound is an essential precursor, partly because it can be photoexcited to substantially enhance activity compared to thermal catalysis, but it also affords the opportunity for direct mechanistic analysis [8–10]. Therefore, a revised ligand set on titanium was proposed to yield a Ti–P bond to study the potential insertion of nonpolar substrates. The expected general synthesis, a transmetallation between a titanium(IV) halide and  $\text{R}_2\text{P}^-$  reagent, tends to reduce titanium [11]. Thus, a more robust route involving the protonolysis of a titanium alkyl precursor was explored. The ideal general method is outlined in Scheme 1.



**Scheme 1.** General scheme for the synthesis of titanium phosphido compounds from a simple titanium precursor.

## 2. Results

Treatment of  $(\text{NMe}_2)_3\text{TiCl}$  with 2 equiv. of *N*-*tert*-butyl acetamide in toluene solution affords a dark-red solution. When the solvent and volatile residue are removed and the resultant residue is crystallized from a concentrated *n*-pentane solution, dark-red crystals of the title compound are obtained in a 90% isolated yield (Scheme 2). As seen in Figure 1, the spectra are simple, with characteristic signals in the  $^1\text{H}$  NMR spectrum, including methyl resonances for the dimethylamido ligand ( $\delta = 3.58$ ) and resonances for amidate methyl ( $\delta = 1.67$ ) and *tert*-butyl ( $\delta = 1.16$ ). The  $^{13}\text{C}\{^1\text{H}\}$  NMR spectrum was similarly simple in assignment, drawing particular attention to the amidate carbon resonance at  $\delta = 176.33$ . These data allowed for the assignment of this product and an assessment of purity, which was acceptable for further use.



**Citation:** Seth, D.M., Jr.; Waterman, R. Bis(*N*-*tert*-butylacetamido)(dimethylamido)(chloro)titanium. *Molbank* **2024**, *2024*, M1786. <https://doi.org/10.3390/M1786>

Academic Editor: René T. Boéré

Received: 14 February 2024

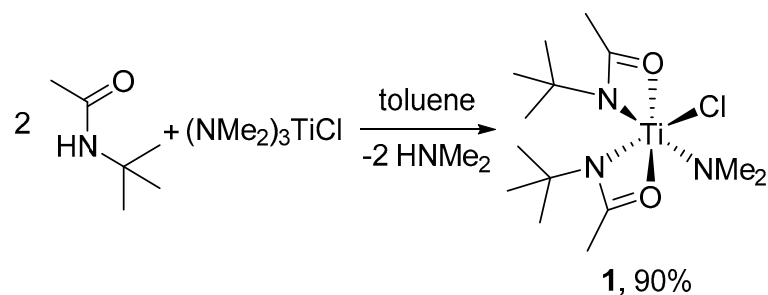
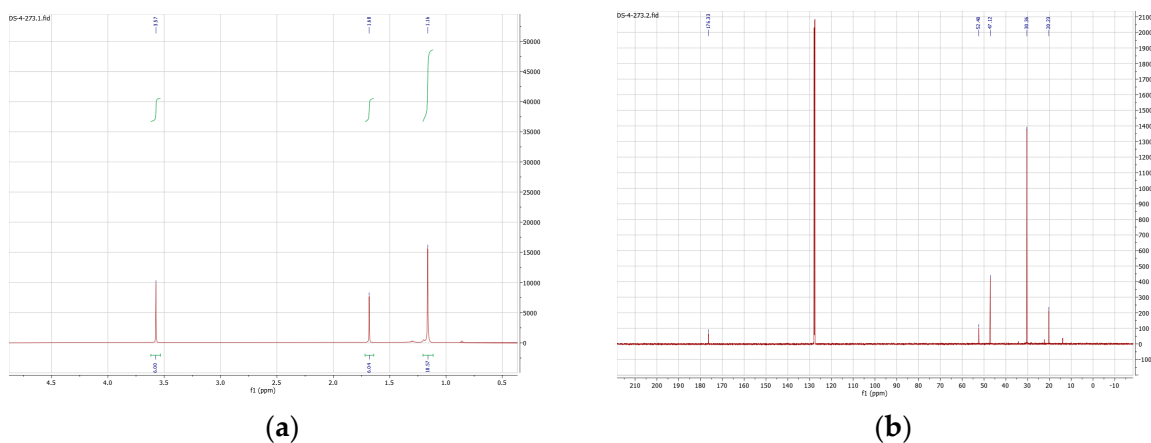
Revised: 1 March 2024

Accepted: 1 March 2024

Published: 6 March 2024

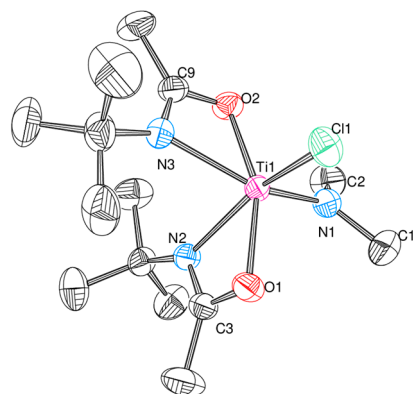


**Copyright:** © 2024 by the authors. Licensee MDPI, Basel, Switzerland. This article is an open access article distributed under the terms and conditions of the Creative Commons Attribution (CC BY) license (<https://creativecommons.org/licenses/by/4.0/>).

Scheme 2. The synthesis of **1**.

**Figure 1.** Representative NMR spectra of compound **1** in benzene- $d_6$  solution. The (a)  $^1\text{H}$  NMR spectrum and (b)  $^{13}\text{C}\{^1\text{H}\}$  NMR spectrum of **1**.

To assign the connectivity of **1**, an X-ray structural study was undertaken. Diffraction-quality plates of **1** formed upon cooling a saturated solution of **1** in *n*-pentane at  $-40^\circ\text{C}$ . The connectivity of this complex is shown in Scheme 3. Selected bond lengths and angles are reported in Table 1. Titanium adopts a pseudo-octahedral geometry with some distortion due to the ancillary ligands' geometry. The short Ti–N bond distance (1.8759(14) Å) and the sum of angles on nitrogen ( $359.7(1)^\circ$ ) for the terminal dimethylamido ligand indicate a significant  $\pi$  donation from nitrogen to titanium. The Ti–N bond distance is similar to bond lengths reported by Schafer in their compound bis(N-2,6-diisopropylphenylpivalamido)bis(dimethylamido)titanium, specifically Ti–N = 1.8778(12) Å [12]. The Ti–Cl bond 2.3142(8) Å of **1** is slightly longer than that reported by Schafer in their compound bis(N-2,6-diisopropylphenylpivalamido)bis(chloro)titanium, which is Ti–Cl = 2.2459(12) Å [12]. This feature may be attributed to the limited  $\pi$  donation of the chloro ligand, which would be a less favorable  $\pi$  donor than the *cis* dimethylamido ligand. Indeed, the Ti–Cl bond length is similar to that reported by Stahl in their (pentamethylcyclopentadienyl)bis(N-phenylacetamido)(chloro)titanium Ti–Cl = 2.358(1) Å [13], which would show a similar limited  $\pi$  donation due to competition from the ancillary Cp\* ligand. Further, an examination of the amidate ligands shows that the Ti–O bond is shorter than the Ti–N bond, which is reflective of titanium's oxophilicity and is in line with previously reported titanium amidates [13–18].



**Scheme 3.** ORTEP rendering of the molecular structure of compound **1**. Thermal ellipsoids are at the 50% probability level.

**Table 1.** Selected bond lengths and angles for **1**.

Distance (Å)		Angle (Degrees)	
Ti1–N1	1.8759(14)	C2–N1–C1	111.85(15)
Ti1–O2	1.9795(12)	C2–N1–Ti1	128.56(12)
Ti1–O1	1.9925(12)	C1–N1–Ti1	119.29(12)
Ti1–N2	2.1921(13)	N1–Ti1–Cl1	100.41(4)
Ti1–N3	2.2052(14)	O2–Ti1–Cl1	106.11(4)
Ti1–Cl1	2.3142(8)	O1–Ti1–Cl1	92.93(3)
Ti1–C3	2.5033(16)	N2–Ti1–Cl1	153.45(4)
Ti1–C9	2.5072(16)	N3–Ti1–Cl1	91.50(4)

### 3. Discussion

The purpose of preparing compound **1** was to advance in the synthetic path outlined in Scheme 1. Unfortunately, compound **1** does not cleanly nor readily react with routine alkylating agents, including <sup>s</sup>BuLi, benzyl potassium, or trimethylsilyl methylolithium. In light of the difficulty in following the early steps in the proposed synthetic pathway, it is apparent that other titanium compounds are doubtlessly more amenable to the proposed protocol. At present, alternative derivatives are under exploration for the aforementioned experiments and application to hydrophosphination catalysis.

### 4. Materials and Methods

(NMe<sub>2</sub>)<sub>3</sub>TiCl was synthesized using the literature methods [19]. NMR spectra were collected using a Bruker AXR 500 MHz spectrometer (Bruker Corporation, Billerica, MA, USA) in a benzene-*d*<sub>6</sub> solution and are reported with reference to residual solvent signals ( $\delta$  = 7.16 and 128.0).

#### 4.1. Synthesis of *N*-*tert*-Butyl Acetamide

Adapted from the literature procedure [20], a 500 mL Schlenk flask was charged with ca. 200 mL of diethyl ether, 9.6 mL of *tert*-butylamine (92 mmol), and 13.4 mL of triethylamine (96 mmol, 1.05 equiv). To this mixture, acetyl chloride (6.3 mL, 88 mmol, 0.96 equiv) was added dropwise, forming a thick colorless precipitate. The solution was stirred for ca. 2 h, after which the reaction mixture was filtered, the solid residue was washed with diethyl ether (2 × 50 mL), and the filtrate and ether washings were combined and concentrated to yield 9.43 g of crude product (93%). The crude product was subjected to recrystallization from a dichloromethane/heptane solvent system to yield 8.7 g off-white/light-pink crystals

(86%). Purity was confirmed by  $^1\text{H}$  NMR spectroscopy, demonstrating that the obtained product yielded matching data to those from the literature preparation used [20].

#### 4.2. Synthesis of $(\text{ON})_2\text{Ti}(\text{NMe}_2)(\text{Cl})$ (1)

In a nitrogen-filled glovebox, a 50 mL round-bottomed flask was charged with 606 mg of  $(\text{NMe}_2)_3\text{TiCl}$  (2.82 mmol), and this was dissolved in ~30 mL of toluene. To this reaction mixture, 657 mg of solid *N-tert-butyl* acetamide was added (5.64 mmol, 2 equivalents) in one portion. The solution rapidly became deep red and was stirred for ca. 22 h, after which the volatile components were removed under reduced pressure to yield a deep-red residue. The residue was redissolved in ~5 mL *n*-pentane, and this solution was kept at  $-40^\circ\text{C}$  for ca. 16 h to yield 902 mg of deep-black-red crystals (2.54 mmol, 90%). Diffraction-quality crystals were obtained from this pentane crystallization.  $^1\text{H}$  NMR (500 MHz):  $\delta$  3.57 (s, 6H, Ti-N( $\text{CH}_3$ )<sub>2</sub>), 1.68 (s, 6H, acetyl- $\text{CH}_3$ ), 1.16 (s, 18H, NC( $\text{CH}_3$ )<sub>3</sub>).  $^{13}\text{C}$  NMR (126 MHz):  $\delta$  176.33, 52.40, 47.12, 30.36, 20.23.

#### 4.3. X-ray Structure Determination

A Bruker APEX 2 CCD platform diffractometer [Mo K $\alpha$  ( $\lambda = 0.71073 \text{ \AA}$ )] was used to collect X-ray diffraction data at 150(2) K. A suitable purple plate was mounted on a MiTiGen Micromount with Paratone-N cryoprotectant oil. Cell refinement and data reduction were performed with SAINT V8.37A [21]. Absorption correction was performed using SADABS-2016/2 [22]. The structure was solved by direct methods and standard difference map techniques and was refined by the least-squares procedure using the ShelXT 2014/15 [23], ShelXL-2018/3 [24], and ShelXle Qt 6.4.0 [25] software packages; the results were visualized with ORTEP [26]. All non-hydrogen atoms were solved anisotropically, and hydrogen atoms were calculated using a riding model.

Crystal data (Supplementary Materials) for  $\text{C}_{14}\text{H}_{30}\text{ClN}_3\text{O}_2\text{Ti}$  ( $M = 355.76 \text{ g/mol}$ ): monoclinic, space group  $C2/c$  (#15),  $a = 29.831(8)$ ,  $b = 10.125(3)$ ,  $c = 14.075(4)$ ,  $\beta = 114.948(3)$ ,  $V = 3854.5(19)$ ,  $Z = 8$ ,  $T = 150(2) \text{ K}$ , MoK $\alpha$  ( $\lambda = 0.71073 \text{ \AA}$ ),  $\rho_{\text{calc}} = 1.226$ ; 22,430 reflections were measured ( $3.01^\circ < 2\theta < 57.41^\circ$  ( $0.74 \text{ \AA}$ )), and 4734 were unique ( $R_{\text{int}} = 0.0511$ ,  $R_{\text{sigma}} = 0.0403$ ), which were used in all calculations. The final  $R_1$  was 0.0325 and  $wR_2 = 0.0903$  ( $I \geq 2\sigma(I)$ ). Full crystallographic information can be found in the Cambridge Crystallographic Data Center, deposit number 2332945.

**Supplementary Materials:** The mol file, cif data and check cif report are available online.

**Author Contributions:** Conceptualization, D.M.S.J. and R.W.; methodology, D.M.S.J.; validation, D.M.S.J. and R.W.; formal analysis, D.M.S.J.; investigation, D.M.S.J.; resources, D.M.S.J.; data curation, D.M.S.J.; writing—original draft preparation, D.M.S.J.; writing—review and editing, R.W.; visualization, D.M.S.J.; supervision, R.W.; project administration, D.M.S.J.; funding acquisition, R.W. All authors have read and agreed to the published version of the manuscript.

**Funding:** This research was funded by NSF, grant number CHE-2101766 (to R.W.).

**Data Availability Statement:** Full crystallographic information can be found in the Cambridge Crystallographic Data Center, deposit number 2332945.

**Acknowledgments:** The authors are grateful for the unwavering support for all efforts in X-ray crystallography from John Hughes, who, despite being a mineralogist, shares our love of big diffracting small molecules.

**Conflicts of Interest:** The authors declare no conflicts of interest.

## References

1. Bange, C.A.; Waterman, R. Challenges in Catalytic Hydrophosphination. *Chemistry* **2016**, *22*, 12598–12605. [[CrossRef](#)]
2. Lau, S.; Hood, T.M.; Webster, R.L. Broken Promises? On the Continued Challenges Faced in Catalytic Hydrophosphination. *ACS Catal.* **2022**, *12*, 10939–10949. [[CrossRef](#)]
3. Novas, B.T.; Waterman, R. Metal-Catalyzed Hydrophosphination. *ChemCatChem* **2022**, *14*, e202200988. [[CrossRef](#)]

4. Perrier, A.; Comte, V.; Moïse, C.; Le Gendre, P. First Titanium-Catalyzed 1,4-Hydrophosphination of 1,3-Dienes. *Chem.—A Eur. J.* **2010**, *16*, 64–67. [[CrossRef](#)]
5. Sakae, R.; Yamamoto, Y.; Komeyama, K.; Takaki, K. Hydrophosphination of Propargylic Ethers with Diphenylphosphine in the Presence of LiHMDS, N-Heterocyclic Carbene, and Ti(NMe<sub>2</sub>)<sub>4</sub>. *Chem. Lett.* **2010**, *39*, 276–277. [[CrossRef](#)]
6. Zhao, G.; Basuli, F.; Kilgore, U.J.; Fan, H.; Aneetha, H.; Huffman, J.C.; Wu, G.; Mindiola, D.J. Neutral and Zwitterionic Low-Coordinate Titanium Complexes Bearing the Terminal Phosphinidene Functionality. Structural, Spectroscopic, Theoretical, and Catalytic Studies Addressing the Ti–P Multiple Bond. *J. Am. Chem. Soc.* **2006**, *128*, 13575–13585. [[CrossRef](#)]
7. Seth, D.M., Jr.; Waterman, R. Photo-Initiated Radical Hydrophosphination at Titanium Compounds Capable of Ti–P Insertion. *Organometallics* **2023**, *42*, 1213–1219. [[CrossRef](#)]
8. Rosenberg, L. Mechanisms of Metal-Catalyzed Hydrophosphination of Alkenes and Alkynes. *ACS Catal.* **2013**, *3*, 2845–2855. [[CrossRef](#)]
9. Waterman, R. Triamidoamine-Supported Zirconium Compounds in Main Group Bond-Formation Catalysis. *Acc. Chem. Res.* **2019**, *52*, 2361–2369. [[CrossRef](#)]
10. Reuter, M.B.; Seth, D.M.; Javier-Jiménez, D.R.; Finfer, E.J.; Beretta, E.A.; Waterman, R. Recent advances in catalytic pnictogen bond forming reactions via dehydrocoupling and hydrofunctionalization. *Chem. Commun.* **2023**, *59*, 1258–1273. [[CrossRef](#)]
11. Normand, A.T.; Bonnin, Q.; Brandès, S.; Richard, P.; Fleurat-Lessard, P.; Devillers, C.H.; Balan, C.; Le Gendre, P.; Kehr, G.; Erker, G. The Taming of Redox-Labile Phosphidotitanocene Cations. *Chem.—A Eur. J.* **2019**, *25*, 2803–2815. [[CrossRef](#)]
12. Horrillo-Martinez, P.; Leitch, D.C.; Ryken, S.A.; Thomson, R.K.; Beard, J.D.; Patrick, B.O.; Schafer, L.L.; Giesbrecht, G.R. Titanium amidate complexes as active catalysts for the synthesis of high molecular weight polyethylene. *Can. J. Chem.* **2015**, *93*, 775–783. [[CrossRef](#)]
13. Kissounko, D.A.; Guzei, I.A.; Gellman, S.H.; Stahl, S.S. Titanium(IV)-Mediated Conversion of Carboxamides to Amidines and Implications for Catalytic Transamidation. *Organometallics* **2005**, *24*, 5208–5210. [[CrossRef](#)]
14. Lee, A.V.; Schafer, L.L. Modular N,O-Chelating Ligands: Group-4 Amidate Complexes for Catalytic Hydroamination. *Eur. J. Inorg. Chem.* **2007**, *2007*, 2245–2255. [[CrossRef](#)]
15. Zhang, Z.; Schafer, L.L. Anti-Markovnikov Intermolecular Hydroamination: A Bis(amidate) Titanium Precatalyst for the Preparation of Reactive Aldimines. *Org. Lett.* **2003**, *5*, 4733–4736. [[CrossRef](#)]
16. Zhang, Z.; Leitch, D.C.; Lu, M.; Patrick, B.O.; Schafer, L.L. An Easy-To-Use, Regioselective, and Robust Bis(amidate) Titanium Hydroamination Precatalyst: Mechanistic and Synthetic Investigations toward the Preparation of Tetrahydroisoquinolines and Benzoquinolizine Alkaloids. *Chem.—A Eur. J.* **2007**, *13*, 2012–2022. [[CrossRef](#)]
17. Bexrud, J.A.; Eisenberger, P.; Leitch, D.C.; Payne, P.R.; Schafer, L.L. Selective C–H Activation  $\alpha$  to Primary Amines. Bridging Metallaaziridines for Catalytic, Intramolecular  $\alpha$ -Alkylation. *J. Am. Chem. Soc.* **2009**, *131*, 2116–2118. [[CrossRef](#)] [[PubMed](#)]
18. Thomson, R.K.; Zahariev, F.E.; Zhang, Z.; Patrick, B.O.; Wang, Y.A.; Schafer, L.L. Structure, Bonding, and Reactivity of Ti and Zr Amidate Complexes: DFT and X-Ray Crystallographic Studies. *Inorg. Chem.* **2005**, *44*, 8680–8689. [[CrossRef](#)]
19. Benzing, E.; Kornicker, W. Dialkylamido-titan(IV)-chloride und -alkoholate. *Chem. Ber.* **1961**, *94*, 2263–2267. [[CrossRef](#)]
20. Catherall, A.L.; Hill, M.S.; Johnson, A.L.; Kociok-Köhn, G.; Mahon, M.F. Homoleptic zirconium amidates: Single source precursors for the aerosol-assisted chemical vapour deposition of ZrO<sub>2</sub>. *J. Mater. Chem. C* **2016**, *4*, 10731–10739. [[CrossRef](#)]
21. Bruker AXS Inc. *SAINT v8. 37A*; Bruker AXS Inc.: Singapore, 2015.
22. Krause, L.; Herbst-Irmer, R.; Sheldrick, G.M.; Stalke, D. Comparison of silver and molybdenum microfocus X-ray sources for single-crystal structure determination. *J. Appl. Crystallogr.* **2015**, *48*, 3–10. [[CrossRef](#)] [[PubMed](#)]
23. Sheldrick, G. SHELXT: Integrating space group determination and structure solution. *Acta Crystallogr. Sect. A* **2014**, *70*, C1437. [[CrossRef](#)]
24. Sheldrick, G.M. Crystal structure refinement with SHELXL. *Acta Crystallogr. Sect. C-Struct. Chem.* **2015**, *71*, 3–8. [[CrossRef](#)] [[PubMed](#)]
25. Hubschle, C.B.; Sheldrick, G.M.; Dittrich, B. ShelXle: A Qt graphical user interface for SHELXL. *J. Appl. Crystallogr.* **2011**, *44*, 1281–1284. [[CrossRef](#)]
26. Farrugia, L.J. WinGX and ORTEP for Windows: An update. *J. Appl. Crystallogr.* **2012**, *45*, 849–854. [[CrossRef](#)]

**Disclaimer/Publisher’s Note:** The statements, opinions and data contained in all publications are solely those of the individual author(s) and contributor(s) and not of MDPI and/or the editor(s). MDPI and/or the editor(s) disclaim responsibility for any injury to people or property resulting from any ideas, methods, instructions or products referred to in the content.